Electrochimica Acta 465 (2023) 142997

Contents lists available at ScienceDirect

Electrochimica Acta

journal homepage: www.journals.elsevier.com/electrochimica-acta

Cathodic stripping of elemental Te in dichloromethane

D.A. Cook, S.J. Reeves, W. Zhang, G. Reid, W. Levason, P.N. Bartlett *

School of Chemistry, University of Southampton, Highfield, Southampton SO17 1BJ, United Kingdom

ARTICLE INFO

Keywords:
Tellurium
Chlorometallate
Stripping
Non-aqueous
Te(-II)

ABSTRACT

The cathodic stripping of Te in CH_2Cl_2 with 0.1 M $[N^nBu_4]Cl$ has been studied. In background electrolyte the cathodic stripping of Te behaves in the expected way. In contrast, when the stripping occurs in the $[N^nBu_4]_2[TeCl_6]$ plating solution, unusual voltammetry is observed. Microelectrode and EQCM studies show that cathodic stripping of Te in the plating solution occurs with the passage of very little charge and leads to the formation of Te(0) in solution due to a rapid reaction between the reduced Te(-II) species and the Te(IV) salt. As a result, the limiting current for reduction of the Te(IV) is unchanged with 4 electron reduction leading to the formation of Te (0) on the electrode at potentials positive of the Te cathodic stripping potential and Te(0) in solution at potentials negative of the Te cathodic stripping potential. The same behaviour is found when a Te(II) precursor is used in place of the Te(IV) salt.

1. Introduction

In its bulk form at room temperature tellurium is a narrow (~0.35 eV) bandgap p-type semiconductor with a unique crystal structure in which the Te atoms are linked in infinite triangular helical chains held together by van der Waals interactions [1]. Consequently, Te has a propensity for 1D growth and forms a variety of interesting nanostructures [2]. Te has the configuration $5s^25p^4$ with the two paired s-electrons lying at lower energy compared to the four p-electrons that occupy the three p-orbitals and account for the anisotropic properties of elemental Te. Te is also an important constituent of a number of semiconducting compounds and alloys that have useful and important electrical properties and find application in many electronic technologies and devices, including phase-change memory, thermoelectrics, and photoconducting and photoelectric devices [3–8]. Consequently, the electrochemical deposition of Te and its compounds and alloys is of interest. For a number of these materials, such as $GeTe_x$ or GST (GeSbTe), electrodeposition requires large negative potentials [9,10] and therefore the use of non-aqueous solvents. At large negative potentials Te(0) can also be reduced to Te(-II) and therefore it is necessary to understand this cathodic reaction which can lead to the stripping of Te(0) from the electrode surface.

In this paper we present results for the cathodic stripping of Te(0) in dichloromethane (CH_2Cl_2) using microelectrodes and EQCM measurements and propose a mechanism for the reaction. A detailed discussion of the electrodeposition of Te from CH_2Cl_2 and the anodic stripping of elemental Te can be found in our earlier paper [11] and in two papers by Liftman et al. [12,13].

2. Experimental

2.1. Preparation of tellurium reagents

The preparation of $[N^nBu_4]_2[TeCl_6]$ and $[NEt_4]_2[TeI_4]$ are described in our previous paper [11]. Briefly, $[N^nBu_4]_2[TeCl_6]$ was prepared from $TeCl_4$ by mixing with $[N^nBu_4]Cl$ in thf, then collecting and purifying the yellow precipitate. The $[NEt_4]_2[TeI_4]$ was made by reaction of elemental Te and I_2 in refluxing CH_3CN followed by addition of $[NEt_4]I$ and subsequent purification. Both products were fully characterised (elemental analysis, ^{125}Te NMR, Raman and IR spectra) and were prepared freshly and stored in an inert atmosphere.

2.2. Electrochemistry

All experiments were carried out in a three-electrode system using an Autolab potentiostat (μAUT70706 Type III) in a recirculating glovebox (Belle Technology, UK). A Pt mesh was employed as the counter electrode and Ag/AgCl (0.1 M $[N^nBu_4]Cl$ in CH_2Cl_2) was used as the reference electrode. $[N^nBu_4]Cl$ (Sigma-Aldrich, ≥99.0%) was kept in the glovebox and used as received. All electrolyte solutions were prepared using anhydrous CH_2Cl_2 (Sigma-Aldrich, 95%, dried by refluxing with CaH_2, distilled and stored in the glovebox).

* Corresponding author.
E-mail address: pnb@soton.ac.uk (P.N. Bartlett).

https://doi.org/10.1016/j.electacta.2023.142997
Received 3 May 2023; Received in revised form 5 August 2023; Accepted 7 August 2023
Available online 8 August 2023

Working electrodes were either 0.5 mm, 25 μm or 50 μm diameter Pt wire sealed in glass. They were cleaned before use by polishing with alumina powders (1, 0.3 and 0.05 μm, Buehler, Germany) on a polishing pad (Microcloth, Buehler) with water and dried with a flow of argon prior to use. EQCM measurements were made using Stanford Research Systems QCM200 using 5 MHz At-cut Pt coated quartz crystals with a working electrode diameter of 1.3 cm.

3. Results

3.1. Cathodic stripping of Te in $[N^nBu_4]_2[TeCl_6]$ solution

During electrodeposition of Te from $[N^nBu_4]_2[TeCl_6]$ in dichloromethane a sharp spike in the reduction current is observed at negative potentials once the deposition of Te has started [11]. This similar feature is seen in the literature for Te deposition from other non-aqueous solutions [14–20] and has been assigned to the reduction to Te(-II). At the microdisc electrode it is striking, and significant, that the plateau current for $[TeCl_6]^{2-}$ reduction is identical before and after the sharp reduction spike and that the charge passed in the spike is very small compared with the charge passed in reduction of $[TeCl_6]^{2-}$ (Fig 1 and SI Fig S1).

In some cases, multiple spikes are observed (see SI, Fig S2) and on repeat scans (not shown) the reduction spikes are not always at precisely the same potential, but the spikes only occur once reduction of $[TeCl_6]^{2-}$ has started and the current before and after the spike is the same. This effect is also seen on macroelectrodes (see SI Fig S3), although now the reduction spike is not as sharp, presumably due to the slower response time caused by the increased double layer capacitance and larger uncompensated resistance.

3.2. EQCM study

We have used EQCM measurements to determine where the deposition of Te onto the electrode occurs and the potential regions where the stripping of deposited Te(0) to solution soluble species occurs. Compared to the voltammetry at the microelectrode, the response on the larger EQCM electrode is significantly more drawn out on the potential scale due to the much larger iR drop. Nevertheless, the cathodic stripping spike can be seen at -2.7 V just after the peak in the deposition voltammogram at -2.5 V, Fig. 2.

Reduction of $[TeCl_6]^{2-}$ starts from +0.6 V on the negative scan but the mass only starts to increase from around -0.5 V, consistent with the initial reduction of $[TeCl_6]^{2-}$ to a soluble Te(II) species as found in rotating ring disc experiments in our previous work [11]. Beyond -0.5 V the mass and reduction current increase until at -2.6 V the mass suddenly significantly decreases as the Te deposit is reductively stripped from the electrode surface. This stripping is associated with a small peak in the reduction current, but not with a significant reduction charge, Fig. 2. On the return scan the mass continues to drop slowly until -2.1 V, even although the reduction of $[TeCl_6]^{2-}$ continues throughout. Scanning positive from -2.1 V the mass now increases steadily as Te(0) is again deposited on the electrode, until +0.6 V on the anodic scan. Beyond +0.6 V anodic stripping of Te(0) begins and the mass falls back close to its starting value. In contrast to the cathodic stripping the anodic stripping is associated with the passage of a significant charge, Fig. 2.

The EQCM data were analysed using the Sauerbrey equation assuming that the deposit was smooth and rigid [21]. For the 5 MHz AT cut quartz crystal at 19°C, the conversion factor is 56.6 Hz cm^{-1} μg^{-1}. Plotting the calculated mass changes against the charge passed, Fig. 2B, clearly shows that the deposition of elemental Te is a 4-electron process and occurs on the negative scan between -1.24 and -2.45 V and again on the positive scan between -1.61 and -0.25 V. The anodic stripping of Te under these conditions at potentials positive of +0.96 V is also a 4-electron process corresponding to

$$Te(0) + nCl^- \rightarrow [TeCl_n]^{-(n-4)} + 4e^- \quad (1)$$

From the EQCM results it is clear that cathodic stripping of Te occurs at potentials more negative than -2.6 V in this experiment and that it is associated with the spike in reduction current, but that the charge passed in the reduction spike is much less that the charge required to strip the deposited tellurium according to the reaction

$$Te(0) + 2e^- \rightarrow Te^{2-} \quad (2)$$

It is also clear from Fig. 2 that the cathodic stripping of Te in the $[TeCl_6]^{2-}$ solution does not remove all of the deposited Te from the electrode surface as the mass only falls to around 0.75 μg cm^{-2} (corresponding to the equivalent of ~3 monolayers of Te) until -1.8 V on the return positive scan when the mass starts to increase again.

3.3. Cathodic stripping of Te in $[NEt_4]_2[TeI_4]$ solution

Essentially the same cathodic stripping process is seen in the deposition of Te from the Te(II) source, $[TeI_4]^{2-}$ in 0.1 M $[N^nBu_4]Cl$ supporting electrolyte (under these conditions the $[TeI_4]^{2-}$ is expected to undergo rapid exchange of the halide ligands to produce $[TeCl_4]^{2-}$).

For the Te(II) precursor, the cathodic stripping feature occurs at the same potential as the cathodic stripping of deposited Te in a 0.1 M $[N^nBu_4]Cl$ solution (see below). The charge passed in the cathodic stripping is again less that charge passed in Te deposition and the current returns to exactly the same limiting current corresponding, in this case, to a 2-electron reduction.

The same behaviour is seen at a macroelectrode (see SI, fig S5) and EQCM experiments again confirm deposition of Te during the cathodic scan (see SI, fig S6).

3.4. Cathodic stripping of tellurium in background electrolyte

Fig. 4 (and SI Fig S7) shows CVs of Te coated electrodes in an electrolyte with no tellurium-containing salt. Each electrode had a different charge passed during the deposition of Te and therefore a different amount of Te coating. The onset potential for the reduction is the same for each electrode, and the current initially increases in the same way but the peak potential changes depending on the amount of material initially present on the electrode. This is all consistent with the classical peak behaviour expected for metal stripping, however in this case it is a cathodic stripping process rather than anodic.

The total charge passed in the cathodic stripping reaction was found to be ~ 50 % of the Te deposition charge, Table 1 (and SI Table S1), consistent with 4-electron deposition of Te in the Te(IV) solution and 2-electron stripping of Te in the background electrolyte, as described by reaction (2). In this case, where there is no Te(IV) or Te(II) in solution, the entirety of the Te coating is reductively stripped.

4. Discussion

Reviews of the early studies of Te electrochemistry can be found in the literature [22,23] and have their origins in the early days of polarography [24]. Initial studies were carried out at mercury electrodes in aqueous solution where complexation of Te with oxygen and the solution pH have a significant effect on the speciation of the Te(IV), Te(II) and Te(-II) oxidation states. Lingane and Niedrach reported sharp

Table 1
Charges associated with the cathodic stripping of Te in 0.1 M $[N^nBu_4]Cl$ in CH_2Cl_2, conditions as in Fig. 4.

Q_{plate} / μC	Q_{strip} / μC	Q_{strip}/Q_{plate} ratio
181	95.0	0.53
101	52.0	0.52
38.1	15.7	0.41

maxima on the polarographic diffusion current plateau for reduction of Te(IV) in acidic citrate buffer coincident with the Te(0)/Te(-II) half wave potential and observed the formation of brown turbidity in solution which they attributed to elemental Te. They suggested that the maxima were due to streaming, i.e. motion of the Hg surface caused by electrocapillary effects, and enhanced mass transport in the solution. They noted that at potentials both before and after the sharp maxima the current was the same and corresponded to diffusion limited, 4-electron reduction of Te(IV) which remained unexplained. Subsequently Schmidt and von Stackelberg [25] showed that for TeO_3^{2-} in NH_3/NH_4Cl at pH 10 the reduction gave a 4-electron wave at the dropping mercury electrode whereas in 0.1 M NaOH at pH 13 the reduction gave a 6-electron wave. In this work they saw only a small maximum in the presence of a surface active species (gelatin) at a potential corresponding to the Te(0)/Te(-II) couple which they attributed to streaming at the mercury surface. They explained the "abnormal polarograms" obtained at pH 10 in which the Te(IV) undergoes 4-electron reduction at potentials both positive and negative of the Te(0)/Te(-II) couple as the results of very rapid reaction between Te(-II) and Te(IV) species in the diffusion layer leading to precipitation of Te(0) in solution

$$2Te(-II) + Te(IV) \rightarrow 3Te(0) \quad (3)$$

In 0.1 M NaOH they propose that 6-electron reduction of Te(IV) is seen because reaction (3) is slow and occurs outside the diffusion layer, in the solution bulk. Gokhshtein [26] studied $[TeO_3]^{2-}$ reduction in 1M NH_3Cl, 1M NH_4OH at a stationary mercury drop. They observed a sharp maximum in the limiting current region and found that the charge associated with this maximum was one half of that corresponding to the Te(IV) reduction wave, consistent with reduction of Te(0) to Te(-II).

In 1969 Jamieson and Perone [27] re-examined the voltammetry of Te(IV) in aqueous alkaline solutions at the hanging mercury drop electrode and their paper provides an in depth comparison to the earlier literature. They conclude that both Schmidt and von Stackelberg [25] and Lingane and Niedrach [28] were partially correct in that the maximum is primarily due to reduction of Te(0) to Te(-II), and that in moderately alkaline solutions the Te(-II) reacts with Te(IV) to produce Te(0) in the diffusion layer (reaction (3) above) but there was also regular pulsing in the current on a slow timescale consistent with the work of Lingane and Niedrach. Subsequently Shinagawa *et al.* [29] highlighted the protonation of the Te(-II) in solution to form HTe^- and the catalytic effect of Te on the evolution of hydrogen at the mercury electrode.

More recent work has extended to the study of Te deposition in ionic liquids [14–20] and for deposition from neutral and acidic aqueous solutions [23,27–32] (see SI and Figs S8-S10). Again, in these studies a clear maximum is seen on the reduction scan with the current returning to a value consistent with 4-electron reduction of Te(IV) both before and after the maximum.

For dichloromethane our results show that the cathodic stripping of Te in background electrolyte (Fig. 4) behaves exactly as one would expect, with the charge passed corresponding to 2-electron stripping of the Te as Te(-II). In contrast, the cathodic stripping of Te in a Te(IV) or Te(II) plating solution behaves in an unusual way. At the microdisc the cathodic stripping peak is very sharp, and the charge passed is insufficient to account for loss of material by reduction to soluble Te(-II). In addition, the mass transport limited current for reduction is identical before and after the stripping spike and does not show the expected 50% increase expected for a 4-electron reduction of Te(IV) to Te(0) being replaced by 6-electron reduction of Te(IV) to Te(-II) (Fig. 1), or the 100% increase expected in the Te(II) case if the 2-electron reduction of Te(II) to Te (0) gives way to a 4-electron reduction of Te(II) to Te(-II) (Fig. 3). These effects are particularly clear at microelectrodes where steady state mass transport limited currents are obtained, and the electrode response is fast due to the low value of *RC* (the product of the uncompensated resistance and double layer capacitance) but the effects are also evident

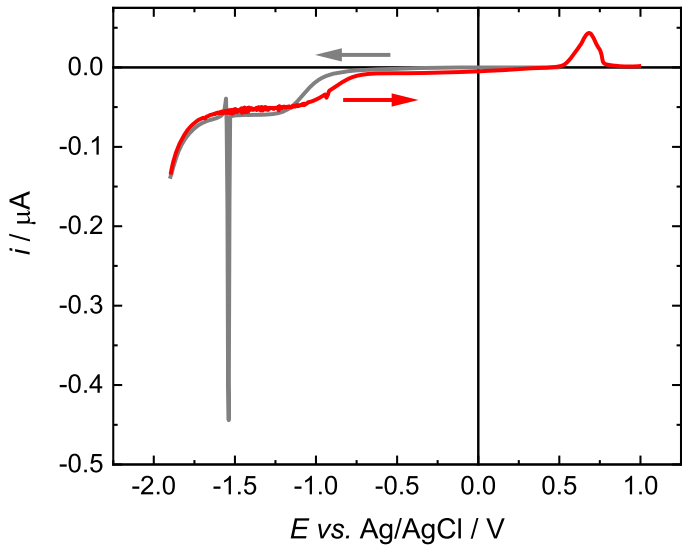

Fig. 1. Cyclic voltammetry in 3.88 mM $[N^nBu_4]_2[TeCl_6]$ in CH_2Cl_2 with 0.1 M $[N^nBu_4]Cl$ at 22°C, using a freshly polished 25 µm diameter Pt disc electrode; sweep rate 50 mV s^{-1}. Grey: cathodic scan; red: anodic scan.

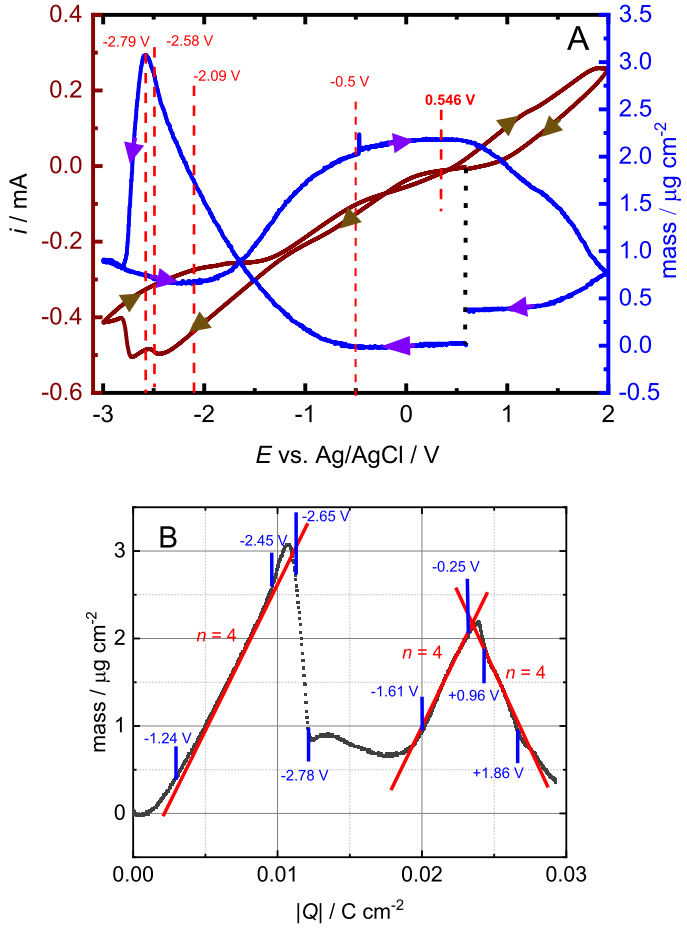

Fig. 2. (A) EQCM results for 2 mM $[N^nBu_4]_2[TeCl_6]$ in CH_2Cl_2 with 0.1 M $[N^nBu_4]Cl$. Pt EQCM electrode diameter 1.3 cm, 19°C, scan rate 50 mV s^{-1}. (B) plot of mass against charge, calculated from A. The red lines are calculated for $n = 4$, the blue lines indicate the different potentials.

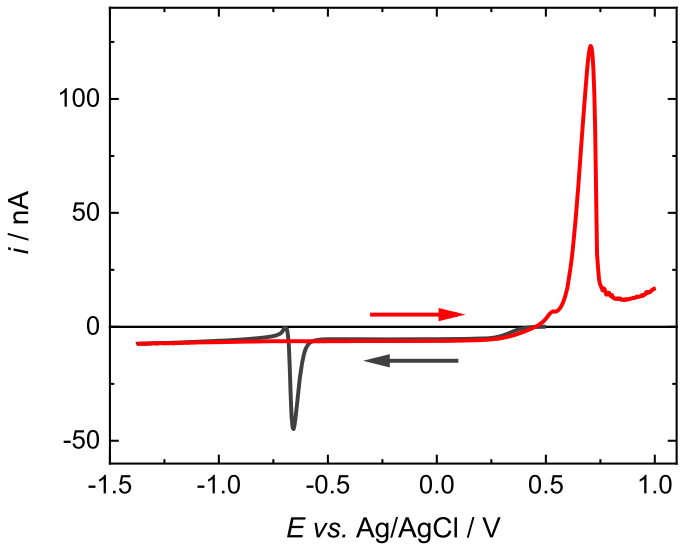

Fig. 3. Cyclic voltammetry in 0.74 mM $[NEt_4]_2[TeI_4]$ in CH_2Cl_2 containing 0.1 M $[N^nBu_4]Cl$. 25 μm diameter Pt microelectrode, scan rate 50 mV s^{-1}.

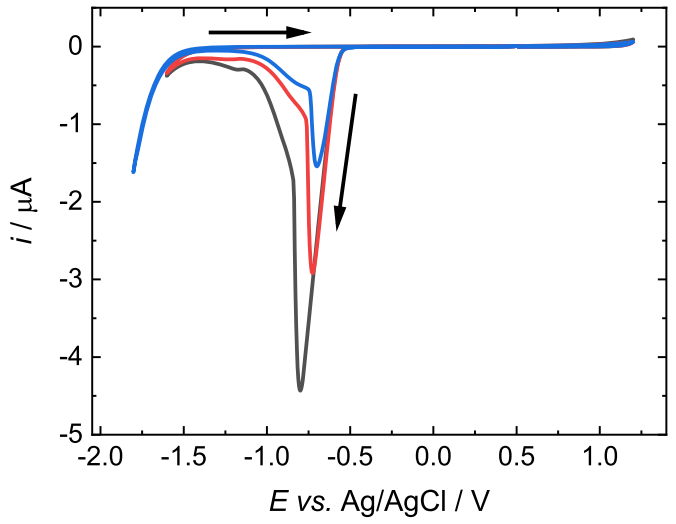

Fig. 4. Cathodic stripping of Te in 0.1 M $[N^nBu_4]Cl$ in CH_2Cl_2. Te coated Pt disc electrode, 0.5 mm diameter, scan rate 20 mV s^{-1}. The Te coating was prepared by electrodeposition from 5 mM $[N^nBu_4]_2[TeCl_6]$ in CH_2Cl_2 with 100 mM $[N^nBu_4]Cl$ at -0.15 V with a charge passed of -38 (blue), -101 (red) and -181 μC (black). The Te coated electrode was then removed from the cell, washed with CH_2Cl_2 and placed into the $[N^nBu_4]Cl/CH_2Cl_2$ electrolyte solution.

for macroelectrodes.

Our results for the limiting currents are consistent with the mechanism proposed by Schmidt and von Stackelberg [25], where the stripping of the Te deposit according to

$$Te(0) + 2e- \rightarrow Te(-II) \quad (4)$$

is followed by reaction of Te(-II) with Te(IV) in solution to give Te(0) (reaction (3) above) or in the case of the Te(II) solution

$$Te(-II) + Te(II) \rightarrow 2Te(0) \quad (5)$$

provided that, as pointed out by Schmidt and von Stackelberg, the solution reactions, (3) or (5), are sufficiently fast that they go to completion within the diffusion layer and no Te(-II) escapes to the bulk solution. In the case of the microdisc, taking a reasonable estimate for the diffusion coefficient of the Te(-II) species of 8×10^{-6} cm^2 s^{-1} [11], this implies that second order rate constant for this reaction must be $>10^7$ dm^{-3} mol^{-1} s^{-1} based on an estimate of the reaction layer thickness and the electrode radius.

According to this mechanism the overall reaction for the stripping of Te(0) in the presence of Te(IV) can be written (by combining reactions (3) and (4)) as

$$Te(0) + 4e + Te(IV) \rightarrow 2Te(0) \text{ in solution} \quad (6)$$

which explains why the cathodic stripping of Te(0) in the plating solution occurs with passage of very little charge.

A notable feature of the microelectrode voltammetry is that the cathodic stripping peak in the Te(IV) plating solution is very sharp (fwhm of around 10 mV, Figs. 1, S1, S2) rather than the more classic stripping profile seen in the Te(II) plating solution (Fig. 3) or the background electrolyte (Fig. 4). For stripping in background electrolyte, cathodic stripping of Te occurs at -0.5 V *vs.* AgCl/Ag, presumably reflecting the thermodynamic potential for reduction of Te(0) to Te(-II) in our solution. For the Te(II) plating solution (Fig. 3) the cathodic stripping occurs at a very similar potential. In contrast, for the Te(IV) solution the the cathodic stripping spike occurs at significantly more negative potentials in the range -1.0 to -1.7 V (Fig. 1 and SI). However, on repeated cycling, if the Te is not stripped anodically from the electrode, the cathodic stripping peak shifts to around -0.5 V (Fig. S4) and is similar in appearance to that for Te stripping in background electrolyte (Fig. 4). This suggests that there is some sort of nucleation process that controls the Te(0) stripping in the Te(IV) solution. Similar sharp surface voltammetry peaks are common in studies of solid molecular redox species on electrode surfaces [33–38]. In these cases the behaviour has been explained in terms of nucleation effects and cooperative interactions in the partially oxidised or reduced surface lattice that decrease the thermodynamic driving force for surface phase transformation [39,40]. It is not clear why this is only seen for the Te(IV) plating solution but it is clear from the repeated spiking seen on cycling (Fig. S2) that at potentials negative of the Te(0) stripping potential, Te (0) is first deposited on the electrode surface and then subsequently stripped from the surface in a rapid pulse.

5. Conclusions

Cathodic stripping of Te in background electrolyte behaves in the normal way in terms of charge passed and shape of the voltammetry and is a 2-electron process in CH_2Cl_2 containing 0.1 M $[N^nBu_4]Cl$.

In contrast, the corresponding reaction in the Te plating solution containing either Te(IV) or Te(II) shows an unusual behaviour because of a very fast homogeneous reaction between the Te(-II) species produced by reduction of the Te on the electrode and the Te(II) or Te(IV) species in solution. This homogeneous reaction leads to cathodic stripping of the Te(0) with the passage of very little charge ($n<<2$) and the formation of dissolved Te(0) in solution. As a result, the limiting current for reduction of the Te(II) or Te(IV) plating reagent is unchanged, with the 2- or 4-electron reduction leading to the formation of Te(0) on the electrode at potentials positive of the Te cathodic stripping potential and Te(0) in solution at potentials negative of the Te cathodic stripping potential.

CRediT authorship contribution statement

D.A. Cook: Conceptualization, Methodology, Writing – review & editing. **S.J. Reeves:** Conceptualization, Methodology, Writing – review & editing. **W. Zhang:** Conceptualization, Methodology. **G. Reid:** Conceptualization, Methodology, Resources, Writing – review & editing, Funding acquisition. **W. Levason:** Conceptualization, Methodology. **P. N. Bartlett:** Conceptualization, Methodology, Writing – review & editing, Funding acquisition, Project administration.

Declaration of Competing Interest

The authors declare that they have no known competing financial interests or personal relationships that could have appeared to influence the work reported in this paper.

Data availability

Data will be made available on request.

Acknowledgments

This work was supported by the EPSRC through the Advanced Devices by ElectroPlaTing program grant (ADEPT; EP/N035437/1).

Supplementary materials

Supplementary material associated with this article can be found, in the online version, at doi:10.1016/j.electacta.2023.142997.

References

[1] A. von Hippel, Structure and conductivity in the VIb group of the periodic system, J. Chem. Phys. 16 (1948) 372–380.
[2] Z. He, Y. Yang, J.W. Liu, S.H. Yu, Emerging tellurium nanostructures: controllable synthesis and their applications, Chem. Soc. Rev. 46 (2017) 2732–2753.
[3] P.G. Guo, A.M. Sarangan, I. Agha, A review of germanium-antimony-telluride phase change materials for non-volatile memories and optical modulators, Appl. Sci. 9 (2019). Basel.
[4] A. Kramer, M.L. Van de Put, C.L. Hinkle, W.G. Vandenberghe, Tellurium as a successor of silicon for extremely scaled nanowires: a first-principles study, NPJ 2D Mater. Appl. 4 (2020).
[5] P. Rani, A.P. Alegaonkar, S.K. Mahapatra, P.S. Alegaonkar, Tellurium nanostructures for optoelectronic applications, Applied Physics a-Materials Science & Processing 128 (2022) 346.
[6] A. Rogalski, HgCdTe infrared detector material: history, status and outlook, Rep. Prog. Phys. 68 (2005) 2267–2336.
[7] Y.X. Shi, C. Sturm, H. Kleinke, Chalcogenides as thermoelectric materials, J. Solid State Chem. 270 (2019) 273–279.
[8] M. Xu, X.L. Mai, J. Lin, W. Zhang, Y. Li, Y.H. He, H. Tong, X. Hou, P. Zhou, X. S. Miao, Recent advances on neuromorphic devices based on chalcogenide phase-change materials, Adv. Funct. Mater. 30 (2020), 2003419.
[9] A.H. Jaafar, L.C. Meng, Y.J. Noori, W.J. Zhang, Y.S. Han, R. Beanland, D.C. Smith, G. Reid, K. de Groot, R.M. Huang, P.N. Bartlett, Electrodeposition of GeSbTe-based resistive switching memory in crossbar arrays, J. Phys. Chem. C 125 (2021) 26247–26255.
[10] G.P. Kissling, R.M. Huang, A. Jolleys, S.L. Benjamin, A.L. Hector, G. Reid, W. Levason, C.H. de Groot, P.N. Bartlett, Electrodeposition of a functional solid state memory material: Germanium antimony telluride from a non-aqueous plating bath, J. Electrochem. Soc. 165 (2018) D557–D567.
[11] D.A. Cook, S.J. Reeves, W. Zhang, G. Reid, W. Levason, P.N. Bartlett, J.M. Dyke, V. K. Greenacre, Tellurium electrodeposition from tellurium(II) and (IV) chloride salts in dichloromethane, Electrochim. Acta 456 (2023), 142456.
[12] Y. Liftman, M. Albeck, Anodic-stripping of tellurium in methylene-chloride, Electrochim. Acta 30 (1985) 381–385.
[13] Y. Liftman, M. Albeck, J.M.E. Goldschmidt, C. Yarnitsky, The electrochemistry of tellurium in methylene-chloride, Electrochim. Acta 29 (1984) 1673–1678.
[14] L.P.M. dos Santos, R.M. Freire, S. Michea, J.C. Denardin, D.B. Araujo, E.B. Barros, A.N. Correia, P. De Lima, Electrodeposition of 1-D tellurium nanostructure on gold surface from choline chloride-urea and choline chloride-ethylene glycol mixtures, J. Mol. Liq. 288 (2019), 111038.
[15] S.I. Hsiu, I.W. Sun, Electrodeposition behaviour of cadmium telluride from 1-ethyl-3-methylimidazolium chloride tetrafluoroborate ionic liquid, J. Appl. Electrochem. 34 (2004) 1057–1063.
[16] E.G.S. Jeng, I.W. Sun, Electrochemistry of tellurium(IV) in the basic aluminum chloride-1-methyl-3-ethylimidazolium chloride room temperature molten salt, J. Electrochem. Soc. 144 (1997) 2369–2374.
[17] A. Sorgho, M. Bougouma, G. De Leener, J. Vander Steen, T. Doneux, Impact of speciation on the tellurium electrochemistry in choline chloride-based deep eutectic solvents, Electrochem. Commun. (2022) 140.
[18] J. Szymczak, S. Legeai, S. Diliberto, S. Migot, N. Stein, C. Boulanger, G. Chatel, M. Draye, Template-free electrodeposition of tellurium nanostructures in a room-temperature ionic liquid, Electrochem. Commun. 24 (2012) 57–60.
[19] L. Thiebaud, S. Legeai, N. Stein, Tuning the morphology of Te one-dimensional nanostructures by template-free electrochemical deposition in an ionic liquid, Electrochim. Acta 197 (2016) 300–306.
[20] R.W. Tsai, Y.T. Hsieh, P.Y. Chen, I.W. Sun, Voltammetric study and electrodeposition of tellurium, lead, and lead telluride in room-temperature ionic liquid 1-ethyl-3-methylimidazolium tetrafluoroborate, Electrochim. Acta 137 (2014) 49–56.
[21] D.A. Buttry, M.D. Ward, Measurement of interfacial processes at electrode surfaces with the electrochemical quartz crystal microbalance, Chem. Rev. 92 (1992) 1355–1379.
[22] A.I. Alekperov, Electrochemistry of selenium and tellurium, Usp. Khim. 43 (1974) 585–611.
[23] S.I. Zhdanov, Chapter 8 tellurium, in: A.J. Bard (Ed.), Encyclopedia of Electrochemistry of the Elements, Vol. IV, Marcel Dekker, New York, 1975, pp. 393–445.
[24] L. Schwaer, K. Suchý, Polarographic studies with the dropping mercury kathode. Part XLV. The electro-reduction of selenites and tellurites, Coll. Czechoslov. Chem. Commun. 7 (1935) 25–32.
[25] H. Schmidt, M. von Stackelberg, The polarographic behaviour of tellurites and tellurates, J. Polarog. Soc. 8 (1962) 49–57.
[26] A.Y. Gokhshtein, Electroreduction of Te(IV) in Alkaline Solution, Polarography 1964, Macmillan, Southampton, 1964, pp. 661–666.
[27] R.A. Jamieson, S.P. Perone, Polarographic, coulometric, and stationary electrode studies of electroreduction of Te(IV) in alkaline solution, J. Electroanal. Chem. 23 (1969) 441–455.
[28] J.J. Lingane, L.W. Niedrach, Polarography of selenium and tellurium .2. The +4 states, J. Am. Chem. Soc. 71 (1949) 196–204.
[29] M. Shinagawa, N. Yano, T. Kurosu, Mechanism and analytical aspects of polarographic maximum wave of tellurium, Talanta 19 (1972) 439–450.
[30] A. Bobrowski, A. Krolicka, J. Sliwa, J. Zarebski, Electrochemical sensing of copper employing tellurium film electrode, Electrochim. Acta 252 (2017) 453–460.
[31] Y.Y. Feng, M. Gu, The electrochemical behavior of tellurium on GCE in sol and solutions, Electrochim. Acta 90 (2013) 416–420.
[32] S.X. Wen, R.R. Corderman, F. Seker, A.P. Zhang, L. Denault, M.L. Blohm, Kinetics and initial stages of bismuth telluride electrodeposition, J. Electrochem. Soc. 153 (2006) C595–C602.
[33] A.M. Bond, S. Fletcher, F. Marken, S.J. Shaw, P.G. Symons, Electrochemical and X-ray diffraction study of the redox cycling of nanocrystals of 7,7,8,8-tetracyano-quinodimethane - Observation of a solid-solid phase transformation controlled by nucleation and growth, J. Chem. Soc. Faraday Trans. 92 (1996) 3925–3933.
[34] A.M. Bond, S. Fletcher, P.G. Symons, The relationship between the electrochemistry and the crystallography of microcrystals. The case of TCNQ (7,7,8,8-tetracyanoquinodimethane), Analyst 123 (1998) 1891–1904.
[35] A.K. Neufeld, I. Madsen, A.M. Bond, C.F. Hogan, Phase, morphology, and particle size changes associated with the solid-solid electrochemical interconversion of TCNQ and semiconducting CuTCNQ (TCNQ = tetracyanoquinodimethane), Chem. Mater. 15 (2003) 3573–3585.
[36] N. Oyama, S. Yamaguchi, T. Shimomura, Analysis for voltammetric responses of molecular-solid tetrathionaphthalene confined on an electrode, Anal. Chem. 83 (2011) 8429–8438.
[37] F. Scholz, M. Lovric, Z. Stojek, The role of redox mixed phases $\{ox_x(C_n\ red)_{1-x}\}$ in solid state electrochemical reactions and the effect of miscibility gaps in voltammetry, J. Solid State Electrochem. 1 (1997) 134–142.
[38] P.N. Bartlett, Some studies of electrodes made from single-crystals of TTF.TCNQ, J. Electroanal. Chem. 300 (1991) 175–189.
[39] S.W. Feldberg, I. Rubinstein, Unusua quasi-reversibility (UQR) or apparent non-kinetic hysteresis in cyclic voltammetry - an elaboration upon the implications of n-shaped free-energy relationships as explanation, J. Electroanal. Chem. 240 (1988) 1–15.
[40] M.J. Yang, R.G. Compton, Voltammetry of adsorbed species: nonideal interactions leading to phase transitions, J. Phys. Chem. C 124 (2020) 18031–18044.